

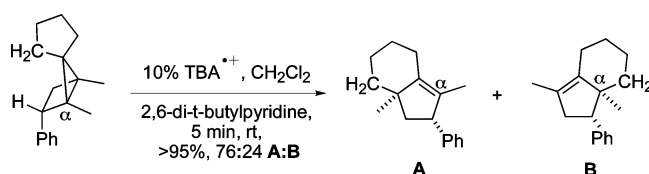
## Remote Substituent Effects upon the Rearrangements of Housane Cation Radicals

James B. Gerken,<sup>†</sup> Selina C. Wang,<sup>‡</sup> Alejandro B. Preciado,<sup>†</sup> Young Sam Park,<sup>†</sup>  
Gisele Nishiguchi,<sup>†</sup> Dean J. Tantillo,<sup>\*,‡</sup> and R. Daniel Little<sup>\*,†</sup>

Department of Chemistry & Biochemistry, University of California—Santa Barbara, Santa Barbara, California 93106, and Department of Chemistry, University of California—Davis, Davis, California 95616

little@chem.ucsb.edu; tantillo@chem.ucdavis.edu

Received January 14, 2005



The rearrangement of a series of housane-derived cation radicals was investigated. Surprisingly, 2-aryl-substituted systems rearranged regioselectively and in a process whose selectivity proved to be independent of the electronic character of para substituents. The major reaction pathway is suggested to be the one that allows maximum delocalization, and allows it to be maintained for as long as possible. Bridging is invoked to account for the regio- and stereoselectivity. When a nonbridging trimethylsilylmethyl substituent is appended to C<sub>2</sub>, the regioselectivity is eroded entirely. B3LYP/6-31G(d) calculations corroborate the notion that bridging plays a role. While bridging ought to stabilize an intermediate by allowing delocalization of the charge/spin, there should be an accompanying entropic penalty. To determine the relative importance of enthalpic and entropic factors in determining the product selectivity, the rearrangement of the *p*-methoxyphenyl-substituted housane was investigated as a function of temperature. Enthalpic factors dominated over the entire temperature range that was explored. Overall, the results indicate that it is possible to influence the direction of migration in housane-derived cation radical rearrangements even when the regiochemical control unit is not directly appended to the migration terminus. This finding suggests that there may be other substituents that can be placed at C<sub>2</sub> that could do the same, perhaps more efficiently.

### Introduction

When oxidized, housanes rearrange to produce cyclopentenes (e.g., **1** to **2**).<sup>1</sup> The reaction proceeds via the removal of an electron from the strained framework to afford a cation radical. The existence of the intermediate has been verified using a number of techniques including ESR.<sup>2</sup> As shown in Scheme 1, a Wagner–Meerwein migration followed by back-electron transfer converts the initial cation radical to the product. As illustrated by the conversion of **3** to **4**, the transformation is regioselective. A substantial body of information indicates that the

electronic properties of the substituents appended to the bridgehead carbons control the regioselectivity.<sup>1,2</sup>

Our interest in this chemistry was kindled by the existence of important mechanistic insights<sup>1,2</sup> and by the desire to explore the use of these interesting processes in synthesis. Our long-standing efforts to devise novel routes to [5.3.0] and [6.3.0] ring systems,<sup>3</sup> coupled with the realization that the oxidatively promoted rearrangement of substrates **6** could, in principle, lead to the assembly of these frameworks (**7–9**), prompted the investigation described herein. Of the several possible ways to assemble housanes, the methodology of Hünig used extensively by Adam and co-workers, seemed most direct and best suited to meet our immediate needs; its

<sup>†</sup> Department of Chemistry & Biochemistry—University of California—Santa Barbara.

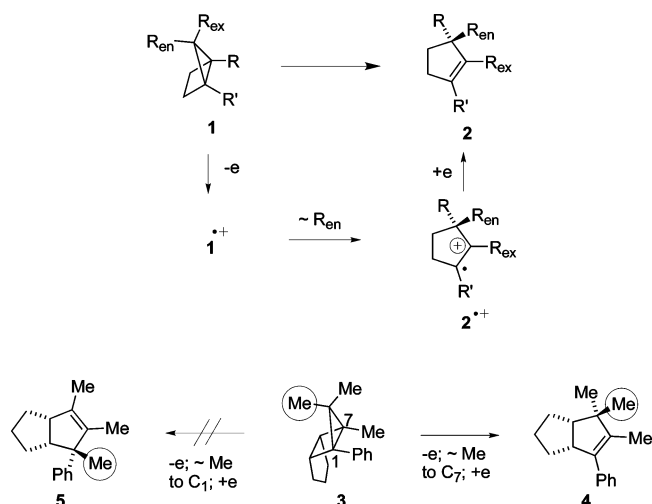
<sup>‡</sup> University of California—Davis.

(1) Adam, W.; Heidenfelder, T. *Chem. Soc. Rev.* **1999**, *28*, 359–365.

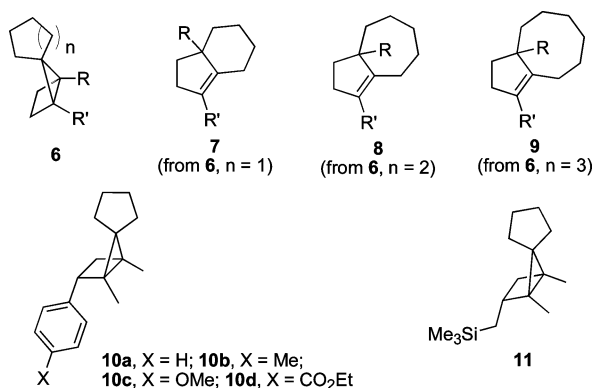
(2) (a) Adam, W.; Sahin, C.; Sendelbach, J.; Walter, H.; Chen, G.-F.; Williams, F. *J. Am. Chem. Soc.* **1994**, *116* (6), 2576–2584. (b) Gerson, F.; Sahin, C. *Helv. Chim. Acta* **2001**, *84* (6), 1470–1488.

(3) (a) Billera, C. F.; Little, R. D. *J. Am. Chem. Soc.* **1994**, *116* (12), 5487–5488. (b) Ott, M. M.; Little, R. D. *J. Org. Chem.* **1997**, *62* (6), 1610–1616. (c) Carroll, Georgia L.; Allan, A. K.; Schwaebe, M. K.; Little, R. D. *Org. Lett.* **2000**, *2* (16), 2531–2534. (d) Mikesell, P. J.; Little, R. D. *Tetrahedron Lett.* **2001**, *42* (25), 4095–4097.

## SCHEME 1



use afforded access to housanes **10a–d** and **11**.<sup>4</sup> Their chemistry, described below, provided unanticipated results.

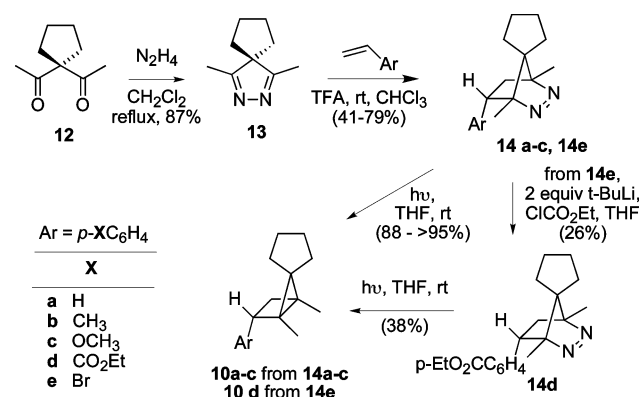


## Results and Discussion

**Synthesis of the Starting Materials.** The key transformations of the Hünig chemistry, illustrated in Scheme 2, involve the reaction of a 1,3-diketone with hydrazine hydrate, followed by a stereospecific, acid promoted, inverse-electron-demand Diels–Alder reaction of the resulting isopyrazole with a suitable dienophile.<sup>4</sup> Unfortunately, the number of “suitable” alkenes is limited.

While Hünig and co-workers were able to expand the scope of the cycloaddition by operating at elevated pressures,<sup>5</sup> we sought to do so while operating at atmospheric pressure. Simple quantum calculations proved useful in guiding our selection of systems to be studied. In particular, we calculated the energy and eigenfunction corresponding to the HOMO for a series of alkenes at the AM1 level. From these results coupled with experiment, we formulate the following guidelines:<sup>6</sup> (a) When  $E_{HOMO}$  is more negative than  $-10$  eV, cycloaddition does not occur. Thus, phenyl vinyl sulfone ( $-10.19$ ), vinyltrimethylsilane ( $-10.24$ ), and allyl bromide ( $-10.35$ ) all failed to react with the protonated isopyrazole **15**. (b)

## SCHEME 2

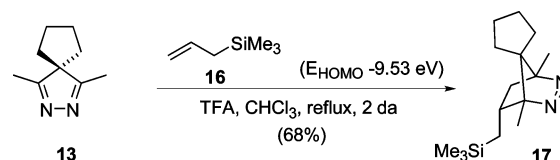


When  $E_{HOMO}$  resides between  $-8.5$  and  $-9.6$  eV, cycloaddition occurs. *p*-Methoxystyrene ( $-8.62$ ), *p*-methylstyrene ( $-8.81$ ), styrene ( $-9.00$ ), cyclopentadiene ( $-9.08$ ), and *p*-bromostyrene ( $-9.10$ ) are dienophiles whose HOMOs fulfill this criterion and they undergo cycloaddition.



One must not be too eager to apply the criterion blindly, however. Thus, while  $E_{HOMO}$  for allyl phenyl sulfide is calculated to be  $-8.54$  eV and therefore falls within the specified range, it fails to react. This is easily understood by realizing that the eigenfunction corresponding to the HOMO is heavily localized on sulfur rather than the alkene. Steric factors can also override predictions based exclusively upon an examination of HOMO energies. For example, styrene reacts reasonably efficiently (53–56%), while 1,1-diphenylethylene and  $\alpha$ -methyl styrene fail to undergo cycloaddition despite the fact that the HOMO energy for each dienophile resides within the reactivity window defined above.

One dienophile we discovered to meet our qualitative criteria was allyltrimethylsilane (**16**). We were gratified to find that it and isopyrazole **13** react slowly, but nonetheless efficiently, to undergo cycloaddition when refluxed in the presence of TFA. As is described later in this paper, the significance of this finding centers upon the utility of the C–Si bond.<sup>7</sup>



A series of C-2 aryl-substituted diazenes, **14a–c**, was assembled in the manner portrayed in Scheme 2 and detailed in the Experimental Section. Diazene **14d** required special attention since the Diels–Alder reaction of isopyrazole **13** and the *p*-carboethoxy substituted

(4) Beck, K.; Hünig, S. *Chem. Ber.* **1987**, *120*, 477–483.

(5) Beck, K.; Hünig, S.; Klaerner, F.-G.; Kraft, P.; Artschwager-Perl, U. *Chem. Ber.* **1987**, *120*, 2041–2051.

(6) Calculations were performed at the indicated level of theory using Spartan '02, Wavefunction, Inc.

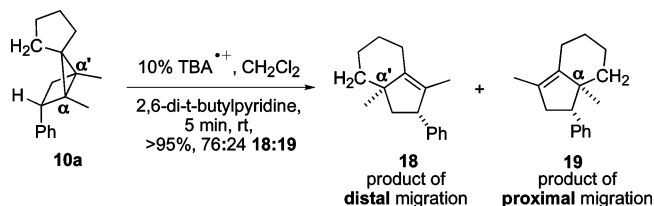
(7) Among a very large number of potential options, consider the following: Lee, T. W.; Corey, E. J. *Org. Lett.* **2001**, *3* (21), 3337–3339. (b) Beignet J.; Cox L. R. *Org. Lett.* **2003**, *5* (22), 4231–4234.

styrene failed. Treatment of the *p*-bromo-substituted diazene **14e** with 2 equiv of *t*-BuLi and ethyl chloroformate, however, provided access to the desired framework **14d**. When irradiated, each diazene was efficiently converted to the corresponding housane, **10a–d**. A UV hand lamp (~365 nm) proved sufficient to effect the transformation, albeit slowly because of the lamp's low intensity; no specialized photochemical equipment was required.

**Selection of the Oxidizing Agent.** Both photoelectron transfer and reagent-induced oxidation of housanes have been shown to afford a cation radical.<sup>1,2</sup> Of the possible oxidizing reagents from which to choose, we selected tris(4-bromophenyl)aminium hexachloroantimonate (TBA<sup>+</sup>;  $E_{\text{ox}} +1.06$  V vs SCE) rather than the more powerful oxidant tris(2,4-dibromophenyl)aminium hexachloroantimonate ( $E_{\text{ox}} +1.50$  V vs SCE).<sup>8</sup> The former has been shown to be capable of oxidizing a variety of housanes, including, for example, 1,4-dimethylbicyclo[2.1.0]pentane and the methyl phenyl tricyclic system **3** ( $E_{1/2}$  1.42 V vs SCE). That it can, despite the fact that the substrates have an oxidation potential more positive than the oxidizing agent, is undoubtedly due to the existence of a fast chemical reaction following the electron-transfer event (e.g., rearrangement), a phenomenon that is often observed in redox-mediated processes.<sup>8,9</sup>

**The Rearrangement.** As indicated in the Introduction, the regioselectivity of the rearrangement of housane cation radicals is governed by the nature of the substituents appended to the bridgehead carbons.<sup>1,2</sup> Our expectation, therefore, was that housanes **10a–d** would not display any selectivity since each bridgehead bears the same substituent. Such was not the case.

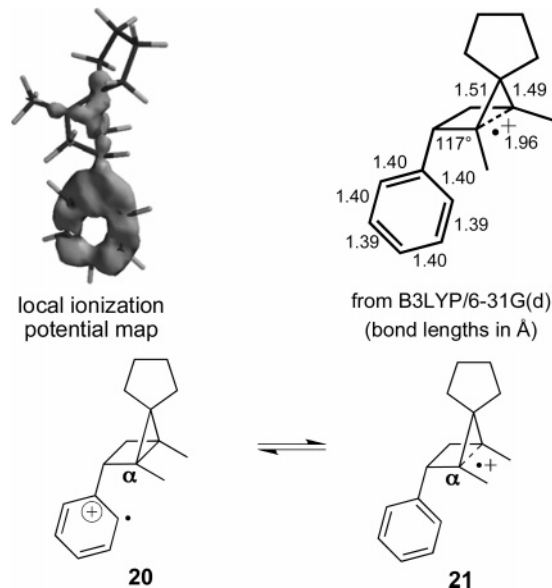
Treatment of housane **10a**, dissolved in dry methylene chloride, with 10 mol % of TBA<sup>+</sup> led to the near-quantitative production of two products, formed in unequal amounts (76:24), after only 5 min at room temperature. Separation, isolation, and characterization confirmed the structures to be **18** and **19**, the former being dominant. Two spectral features greatly simplified the identification process. In the major product (**18**), the benzylic proton is also allylic and therefore appears farther downfield than the benzylic proton in **19** (viz. 3.68 vs 3.18 in **19**). The stereochemical assignment in the minor isomer is also simplified by the fact that the bridgehead methyl group is significantly shielded by the phenyl group located on the adjacent carbon; it appears at 0.6 ppm in **19**. The regio- and stereochemical outcome was confirmed from extensive NOE experiments; details are found in the Supporting Information. Based upon these results, we conclude that there is a preference for migration toward the bridgehead carbon that is distal to the phenyl substituent (viz. toward C<sub>α'</sub> of **10a**).



Molecular mechanics calculations show that **18** is more stable than **19**, and hybrid Hartree–Fock/density func-

tional theory calculations (see the Computational Methods section) show that the cation radical of the major product, **18**, is also more stable than that of **19**, by 1.4 kcal/mol at the B3LYP/6-31G(d) level of theory. Consequently, we wondered whether the product ratio simply reflected thermodynamic control. To address this issue, a sample of the minor adduct, **19**, was resubjected to the reaction conditions. No change was observable by capillary GC analysis after 10 min, 2, 3, or 19 h. We conclude that the products do not interconvert, a result that is consistent with the fact that the cation radicals of **18** and **19** are computed to be 27.4 and 26.0 kcal/mol lower in energy than the initially formed cation radical, and therefore that the ratio does not reflect thermodynamic control.

### SCHEME 3



While the ca. 3:1 preference is not large, it is real and reproducible. One cannot help but wonder why the preference should exist at all. Clearly, the phenyl group, while not positioned at one of the bridgehead carbons, is not an innocent bystander. The phenyl group may be involved in several ways: (a) it may be the site of the initial oxidation, rather than the strained  $\sigma$  framework of the housane, and (b) it may determine both the regio- and stereochemical outcome of the rearrangement by interacting directly with the site of migration. The local ionization potential map illustrated in Scheme 3 is in accord with point a.<sup>10</sup> This map reflects the relative ease of electron removal (ionization) from any location in a

(8) (a) Adam, W.; Sahin, C. *Tetrahedron Lett.* **1994**, 35 (48), 9027–9030. (b) Wend, R.; Steckhan, E. *Electrochim. Acta* **1997**, 42 (13–14), 2027–2039. (c) Steckhan, E. Anodic Oxidation of Nitrogen-Containing Compounds. In *Organic Electrochemistry*, 4th ed.; Lund, H., Hammerich, O., Eds.; Marcel Dekker: New York, 2001; Chapter 15.

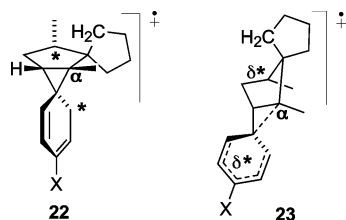
(9) (a) Steckhan, Ed. *Angew. Chem.* **1986**, 98 (8), 681–699. (b) Simonet, J. and Pilard, J.-F., Electrogenerated Reagents. In *Organic Electrochemistry*, 4th ed.; Lund, H., Hammerich, O., Eds.; Marcel Dekker: New York, 2001; Chapter 29. (c) Little, R. D.; Moeller, K. D. *Interface* **2002**, 11 (4), 36–42.

(10) (a) Sjöberg, P.; Murray, J. S.; Brinck, T.; Politzer, P. *Can. J. Chem.* **1990**, 68, 1440–1443 (b) Murray, J. S.; Politzer, P. In *Theoretical Organic Chemistry. Theoretical & Computational Chemistry*; Parkanyi, C., Ed.; Elsevier: Amsterdam, 1998; Vol. 5, p 189. (c) Politzer, P.; Murray, J. S.; Concha, M. C. *Int. J. Quantum Chem.* **2002**, 88, 19–27.

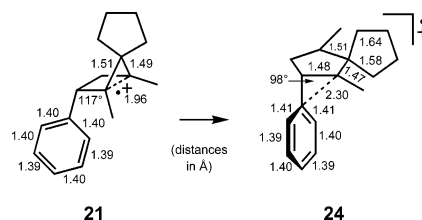
molecule. In this case, both the  $\sigma$  framework and the phenyl group are obviously the most likely candidates. One possibility posits the initial removal of the electron from the aromatic unit to afford a cation radical (**20**) wherein both the charge and odd electron are located there and that this species is in equilibrium with another cation radical (**21**) wherein the charge and odd electron are localized on the strained  $\sigma$  bond that ultimately cleaves. We were able to locate only one [2.1.0] bicyclic cation radical species with B3LYP/6-31G(d) calculations, however, and this species resembles **21** (Scheme 3), not showing any significant delocalization onto the aromatic ring.

To account for the regioselectivity, we invoke the existence of full or partial bridging between the phenyl ring and the bridgehead carbon,  $C_\alpha$ , to afford **22** (fully bridged) or **23** (partially bridged), followed by the preferential movement of the highlighted methylene unit toward the distal bridgehead carbon (*vide infra*) (Scheme 4).<sup>11,12</sup> In addition to providing a rationale for the regioselectivity, the existence of bridging blocks the bottom face of the molecule thereby ensuring that the migration occurs on the opposite side and accounting for the stereochemical outcome that is observed in each of the regioisomers.

## SCHEME 4



B3LYP/6-31G(d) calculations also provide evidence in support of the notion that bridging plays a role. As indicated above, the structure of the first formed cation radical resembles that of the starting material with no indication of involvement by the aryl substituent (**21**). As the reaction proceeds (**21**  $\rightarrow$  **24**), however, the angle between the ipso carbon- $C_2$  and  $C_\alpha$  changes from  $117^\circ$  to  $98^\circ$  as the envelope flattens, thereby suggesting the existence of a bridging interaction.



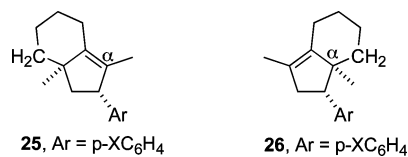
Having made a case for bridging, the question remains: Why should migration toward the *distal* carbon be preferred? After all, bridging stabilizes a species that is common to both paths (see **24**). We suggest that the differences show up after the common intermediate. The major path may simply be the one that allows maximum delocalization, and allows it to be maintained for as long as possible.<sup>13</sup> Migration away from the bridging unit would allow the stabilization to be expressed until such point as it is no longer “needed” (just prior to the back electron transfer?), while migration to the proximal carbon would immediately begin to disrupt bridging and its attendant stabilization, thereby raising the activation barrier for this process.



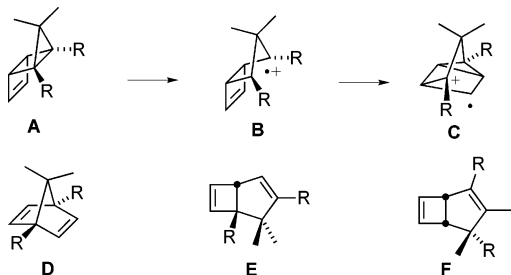
To possibly supply insight into the factors that determine the regioselectivity, we examined the redox chemistry of the para-substituted housanes **10b–d**. When each was subjected to the conditions described previously, rearrangement occurred. The results are summarized in Table 1. Once again, there is a clear preference for the migrating carbon to move *away* from the carbon that we suggest is involved in bridging. Comparison of the two most revealing cases, entry 1 where X is electron withdrawing and entry 4 where it is strongly donating, reveals nearly identical product distributions (80:20 vs 72:28). We conclude that the difference in energy between the transition states for distal and proximal migration is insensitive to the nature of the substituents.<sup>14</sup>

TABLE 1.

entry	X	product ratio ( <b>25/26</b> )	yield (%)
1	CO <sub>2</sub> Et	80:20	87
2	H	76:24	>95
3	CH <sub>3</sub>	76:24	95
4	OCH <sub>3</sub>	72:28	79 (GC)



(11) Adam, W.; Heidenfelder, T.; Sahin, C. *J. Am. Chem. Soc.* **1995**, *117*, 9693–9698. This paper describes an interesting example of bridging in the rearrangement of the housane-derived cation radical **B**. Unlike our system where bridging is invoked to temporarily stabilize the bridgehead carbenium ion, with **B** it leads to the formation of a  $\sigma$ -bond, and ultimately to **D**, **E**, and **F**.



(12) Pioneering studies of aryl bridging can be found in: (a) Cram, D. J. *J. Am. Chem. Soc.* **1952**, *74*, 2129–2137. (b) Cram, D. J. *J. Am. Chem. Soc.* **1964**, *86*, 3767–3772.

(13) (a) Zimmerman, H. E.; Armesto, D. *Chem. Rev.* **1996**, *96* (8), 3065–3112. (b) Hixson, S. S.; Mariano, P. S.; Zimmerman, H. E. *Chem. Rev.* **1973**, *73* (5), 531–551.

TABLE 2.

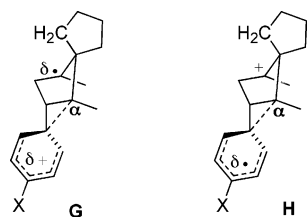
<i>T</i> (K)	25/26	ln(25/26)	10 <sup>3</sup> / <i>T</i>
313	3	1.09	3.195
296	3.5	1.25	3.38
273	4.3	1.45	3.66
233	5.7	1.74	4.29
195	9	2.19	5.13

ever, would be a reduction in degrees of freedom, i.e., there is an entropic penalty associated with bridging that could be manifested differently in the competing transition states leading to the two products.<sup>14b</sup> To determine the relative importance of enthalpic and entropic factors in determining the product selectivity, we investigated the rearrangement of the *p*-methoxy substituted housane **10c** as a function of temperature. The ratio of the major to the minor product, **25/26** (X = OMe), was determined at five different temperatures. The results are summarized in Table 2.

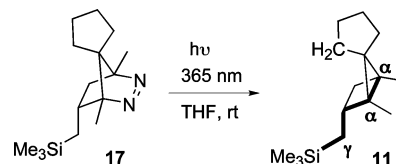
When ln(**25/26**) is plotted as a function of 10<sup>3</sup>/*T*, a straight line results whose slope and intercept are 0.55 and -0.62, respectively. Since ln(**25/26**) = -Δ*H*<sup>‡</sup>/*RT* + Δ*S*<sup>‡</sup>/*R*, it follows that the difference in enthalpies of activation for the competing pathways is -1.09 kcal/mol, while the differences in entropies of activation is only -1.23 eu. The magnitudes of these quantities indicate that enthalpic factors dominate over the entire temperature range that was explored.

**Silylhousane 11.** We wondered how a housane that was devoid of an aryl substituent would behave since its presence, we suggest, is responsible for the selectivity observed in the reactions described thus far. Toward this end, we converted diazene **17** to the trimethylsilylmethylhousane **11** in the manner portrayed in the accompanying equation. A priori, two scenarios appear

(14) (a) At this point, neither of the structures represented by **G** and **H** for the intermediate immediately preceding the alkyl shifts can be definitively ruled out. Previous studies have suggested that the preferred direction of migration for housane cation radicals is, in general, toward the bridgehead that bears the bulk of the positive charge, thus suggesting that **H** may be involved. This view is consistent with the substituent effects described in the text, since both electron-donating and electron-withdrawing substituents stabilize radicals. However, our preliminary B3LYP calculations suggest that **G** best represents the structure formed by ring-opening/flattening of the initially formed housane cation radical. In addition, our calculations suggest that the generalization described above may not correctly predict the preferred direction of migration in some other systems as well. Additional studies are necessary to settle this issue, however, and these will be reported in due course. (b) So far, we have not been able to rationalize the observed regiochemical preferences using our preliminary B3LYP/6-31G(d) calculations. We should note here that it appears that the potential energy surfaces in the vicinity of the housane and "open" cation radicals and the various rearrangement transition structures are rather flat, complicating the analysis. Further explorations using other theoretical methods (including attempts with CI methods) are in progress. We are also considering the effects of entropy and the possibility of dynamic control. The results of these studies will be reported in due course.

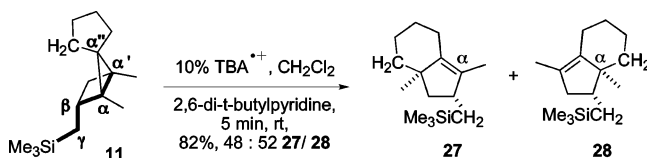


reasonable: (1) The trimethylsilylmethyl group will have no influence upon the regiochemical outcome since it is a nonbridging alkyl substituent and (2) the trimethylsilylmethyl group will serve as the regiochemical control unit and will direct the migration, through the existence of a  $\gamma$ -silyl effect,<sup>15</sup> toward the bridgehead carbon C $\alpha$ .



While the ability of an  $\alpha$ -silyl group to stabilize either a carbanion or a carbenium ion and a  $\beta$ -silyl group to stabilize a carbenium ion is well-known,<sup>16</sup> the capacity of a  $\gamma$ -silyl unit to stabilize intermediates is less appreciated. Whitmore and co-workers first described silicon's stabilizing interaction with a positive charge positioned  $\gamma$  to it in 1946.<sup>15</sup> Since then, many studies have focused upon accelerating effects in solvolysis reactions of systems bearing a 1,3-relationship between a C-Si bond and a leaving group.<sup>17</sup> In general, authors account for dramatic rate increases by invoking the existence of a stabilizing interaction between the back lobe of the  $\gamma$ -C-Si  $\sigma$ -bond and the incipient positive charge. This so-called "percaudal interaction" is maximized when the interacting centers are related by a W-like geometry similar to that highlighted in the structure of the silyl housane **11**,<sup>18</sup> and commonly invoked in discussions of long-range coupling in NMR spectroscopy. The ability of a  $\gamma$ -silyl substituent to stabilize a full or an incipient positive charge should, therefore, direct the rearrangement of **11** so that the methylene unit will migrate toward C $\alpha$ .

When **11** was subjected to the oxidative conditions described previously, nearly equal amounts of **27** and **28** were obtained in an 82% yield. That no regiochemical preference was observed supports the suggestion that full or partial bridging to the aryl substituent controls the regiochemical outcome for the aryl-substituted housanes **10a-d**.



The result also indicates that a  $\gamma$ -silyl effect is not operative, an outcome that appears to be at odds with the commentary presented above. Several factors may

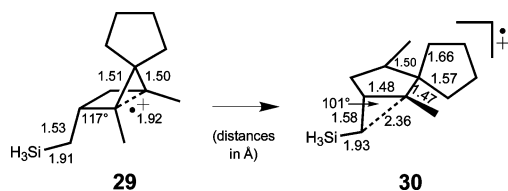
(15) Sommer, L. H.; Dorfman, E.; Goldberg, G. M.; Whitmore, F. C. *J. Am. Chem. Soc.* **1946**, *68*, 488-489. (b) For a review concerning the interaction of silicon with positively charged carbon at the  $\alpha$ ,  $\beta$ ,  $\gamma$ , and  $\delta$  positions see Lambert, J. B. *Tetrahedron* **1990**, *46* (8), 2677-2689.

(16) (a) Ushakov, S. N.; Itenberg, A. M. *Zh. Obshch. Khim.* **1937**, *7*, 2495-2498. (b) Lambert, J. B.; Wang, G.-T.; Finzel, R. B.; Teramura, D. H. *J. Am. Chem. Soc.* **1987**, *109*, 7838-7845. (c) Brinkman, E. A.; Berger, S.; Brauman, J. I. *J. Am. Chem. Soc.* **1994**, *116* (18), 8304-8310.

(17) (a) Green, A. J.; Pigdon, T.; White, J. M.; Yamen, J. *J. Org. Chem.* **1998**, *63*, 3943-3951. (b) Bentley, T. W.; Kirmse, W.; Llewellyn, Söllenböhmer, F. *J. Org. Chem.* **1990**, *55*, 1536-1540. (c) Engler, T. J.; Reddy, J. P. *J. Org. Chem.* **1991**, *56*, 6491-6494.

(18) Kaimakiotis, C.; Fry, A. J. *J. Org. Chem.* **2003**, *68* (26), 9893-9898 reports a novel silicon-aryl effect upon redox potential.

contribute to the absence of an observed  $\gamma$ -silyl effect in this case: (1) a carbenium ion formed at  $C_\alpha$  would be tertiary. In a study appearing in 1999, Tilley and Shiner concluded that tertiary systems do not require, and are consequently not significantly stabilized by,  $\gamma$ -silyl groups.<sup>19</sup> (2) The geometry that is noted by the highlighted bonds in **11** may not correspond to the idealized W-like geometry that is needed for maximum benefit. In fact, by viewing an AM1 geometry-optimized structure of the reactant from the top,<sup>6</sup> one observes that the W-like orientation is accommodated by the  $C_\alpha-C_{\alpha'}$  bond, rather than the  $C_\alpha-C_\beta$  bond that undergoes cleavage. In particular, when the  $C_\gamma-Si$  bond is anti-periplanar to the  $C_\beta-C_\alpha$  bond, as it is in the geometry-optimized structure, the dihedral angle  $C_\gamma-C_\beta-C_\alpha-C_{\alpha'}$  is  $120^\circ$ , while the  $C_\gamma-C_\beta-C_\alpha-C_{\alpha'}$  dihedral angle is a nearly ideal  $178^\circ$ . In addition, the cation radical produced from oxidation of **11** (B3LYP/6-31G(d) with methyls on Si replaced by H's, **29**) shows no significant bending of the  $CH_2SiR_3$  group toward the bridgehead carbon. Interestingly, however, the  $CH_2SiR_3$  group does appear to interact somewhat with this carbon upon conversion to the "open" form of the cation radical (**30**), thereby stabilizing positive charge at that position. Apparently, the regiochemical preference one would expect based on this interaction is somehow overwhelmed, given the regiorandom nature of the transformation.<sup>14b</sup>



## Concluding Remarks

The present study provided surprises at every turn, the most significant being that rearrangement of the 2-aryl-substituted systems occurred regioselectively. Thus, it is possible to influence the direction of migration even when the substituent is not directly appended to the migration terminus. This finding suggests that there may be other substituents that can be placed at  $C_2$  that could do the same, perhaps more efficiently. We are intrigued by functional groups such as OR, SAr, Si(OR) $_3$ , NR $_2$ , and CO $_2$ R since they could stabilize a positive charge at the bridgehead carbon, thereby influencing the regiochemical outcome, and they would also provide a handle for functional and structural modifications. Additional experiments and computations are underway to achieve these objectives and to gain a deeper understanding of the mechanisms and origins of selectivity for these fascinating rearrangements.

## Experimental Section

**General Methods.** Solvents used in reactions were prepared via the following methods. Tetrahydrofuran was distilled from Na/benzophenone, and methylene chloride and acetophenone were distilled from calcium hydride. Chloroform was either distilled from calcium hydride or purchased in predried,

pentene-stabilized form. Basic alumina was purchased from a commercial supplier and dried in an oven heated to  $130^\circ\text{C}$ .

**1,1-Diacetylcyclopentane (Diketone 12).** To 100 mL of DMSO was added 12.412 g (90 mmol) of powdered anhydrous potassium carbonate, followed by 5.0 mL (4.88 g, 49 mmol) of 2,4-pentanedione. The mixture was stirred under argon while 6.5 mL (11.97 g, 55 mmol) of 1,4-dibromobutane was added dropwise over 10 min. The mixture was allowed to stir at room temperature under argon for 24 h, and then 50 mL of brine was added followed by 100 mL of deionized water. The mixture was extracted with  $5 \times 50$  mL of diethyl ether. The combined organic extracts were dried over magnesium sulfate, and the solvent was removed under vacuum. The crude product was then purified via flash chromatography over silica gel in 4:1 hexanes/ethyl acetate. After concentration in vacuo, 4.442 g of **12** was isolated (28.8 mmol, 60%) and determined by GC/MS to be 94% pure. Proton NMR and  $^{13}\text{C}$  NMR data matched the literature values of Beck and Hünig.<sup>4</sup>

**3',5'-Dimethylspiro[cyclopentane-1,4'-[4H]pyrazole] (Isopyrazole 13).** Diketone **12** (3.512 g, 22 mmol) was weighed into a one-necked flask equipped with a water-cooled condenser, a boiling stone, and 11 mL of dry methylene chloride (distilled from calcium hydride). Hydrazine hydrate (1.3 mL, 27 mmol) was added, and the mixture was heated to reflux overnight. The reaction mixture was then allowed to cool, dried over magnesium sulfate, and filtered. The solvent was removed under vacuum to give a white crystalline solid (mp  $111-113^\circ\text{C}$ ) in 2.967 g isolated yield (19.78 mmol, 87%). GC/MS of the product showed no detectable impurities, and NMR data matched the literature values of Beck and Hünig.<sup>4</sup>

**1,4-Dimethyl-anti-5-phenyl-2,3-diazaspiro[bicyclo[2.2.1]heptane-7,1'-cyclopentan]-2-ene (Phenyldiazene 14a).** Isopyrazole **13** (1.026 g, 6.8 mmol) was dissolved in 50 mL of dry chloroform (distilled from calcium oxide) and transferred to a 250 mL round-bottomed flask. Trifluoroacetic acid (0.7 mL, 9.1 mmol) was added with swirling. Styrene (20 mL, 175 mmol) was added, a water-cooled reflux condenser was attached, and the system was purged with argon. The mixture was heated to reflux for 3 days and allowed to cool to ambient temperature. Powdered anhydrous potassium carbonate (2.007 g, 14.5 mmol) was added, and the mixture was stirred at room temperature for 1 h. The mixture was filtered, solvents were removed under vacuum, and the crude product was chromatographed on silica gel in 4:1 hexanes/ethyl acetate. Phenyl diazene **14a** was isolated (973 mg, 3.83 mmol, 56%) as a white powder.

The spectral data were:  $^1\text{H}$  NMR (500 MHz,  $\text{CDCl}_3$ ) 7.2 (m, 3H), 7.0 (m, 2H), 2.94 (dd, 1H), 2.03 (dd, 1H), 1.74 (s, 3H), 1.6–1.3 (m, 10H), 1.2 (m, 2H); NOE enhancements were observed: irradiation at 7.0 ppm led to enhancements at 7.2, 6%; 2.94, 60.67%; 1.74, 2.1%; 1.4, 4.6%; irradiation at 2.94 ppm, afforded enhancements at 7.2, 5.4%; 2.03, 3.3%; 1.5, 12.1%; irradiation at 2.03 ppm, led to enhancements at 2.94, 5.18%; 1.74, 2.08%; 1.5, 5.4%; 1.4, 17.6%;  $^{13}\text{C}$  APT 180.7 (quat), 138.8 (quat), 129.0 (tertiary), 128.0 (tertiary), 126.8 (tertiary), 105.9 (quat), 47.6 (tertiary), 37.5 (secondary), 28.2 (secondary), 26.8 (secondary), 26.6 (secondary), 26.3 (secondary), 13.5 (primary), 11.4 p; IR (neat, attenuated total internal reflectance (ATR)) 3063, 3040, 2948, 2865, 1601, 1495, 1459, 1380, 759, 698  $\text{cm}^{-1}$ ; MS (EI) 226, 211 (base peak), 183, 169, 141, 115, 91, 65, 41; HRMS (CI,  $\text{CH}_4$ ) 255.1854 obsd, 255.1861 calcd for  $\text{C}_{17}\text{H}_{23}\text{N}_2$  ( $\text{M} + \text{H}$ ) $^+$ .

**1,4-Dimethyl-anti-5-(4-methoxyphenyl)-2,3-diazaspiro[bicyclo[2.2.1]heptane-7,1'-cyclopentan]-2-ene (p-Methoxyphenyldiazene 14c).** Isopyrazole **13** (0.750 g, 5 mmol) was dissolved in 5 mL of distilled chloroform. Trifluoroacetic acid (0.34 mL, 4.5 mmol) and 5.0 g (37.5 mmol) of 4-methoxystyrene were added with stirring and heated to reflux. After 42 h, the mixture was allowed to cool to room temperature, 1.295 g (9.4 mmol) of powdered anhydrous  $\text{K}_2\text{CO}_3$  was added, and the mixture was stirred for 35 min. The mixture was filtered, solvents were removed under vacuum, and the crude

(19) Tilley, L. J.; Shiner, V. J., Jr. *J. Phys. Org. Chem.* **1999**, *12*, 564–576.

product was chromatographed in 4:1 hexanes/ethyl acetate. *p*-Methoxyphenyldiazene **14c** was isolated (0.590 g, 2.1 mmol, 41%) as a white powder.

The spectral data were:  $^1\text{H}$  NMR (400 MHz,  $\text{CDCl}_3$ )  $\delta$  6.90 (m, 2H), 6.76 (m, 2H), 3.78 (s, 3H), 2.89 (dd,  $J = 9.2, 5.4$ , 1H), 2.02 (dd,  $J = 13.7, 9.2$ , 1H), 1.72 (s, 3H), 1.7–1.55 (m, 2H), 1.53 (s, 3H), 1.5–1.35 (m, 4H), 1.35 (dd,  $J = 13.7, 5.2$ , 1H), 1.28–1.16 (m, 2H);  $^{13}\text{C}$  NMR (100 MHz,  $\text{CDCl}_3$ ) 158.4, 130.7, 129.8, 113.4, 90.5, 89.9, 67.4, 55.2, 46.7, 37.7, 28.2, 26.7, 26.5, 26.2, 13.4, 11.3; IR (neat) 2953, 1611, 1250, 1033; MS (CI,  $\text{CH}_4$ ) 285, 256, 241, 179, 151 (base peak); HRMS (CI,  $\text{CH}_4$ ) 285.1959 obsd, 285.1967 calcd for  $\text{C}_{18}\text{H}_{25}\text{N}_2\text{O}$  ( $\text{M} + \text{H}$ ) $^+$ .

**1,4-Dimethyl-anti-5-(4-methylphenyl)-2,3-diazaspiro[bicyclo[2.2.1]heptane-7,1'-cyclopentan]-2-ene (*p*-Methylphenyldiazene **14b**).** Isopyrazole **13** (0.722 g, 4.81 mmol) was dissolved in 5.5 mL of chloroform in a round-bottomed flask. Trifluoroacetic acid (0.35 mL, 4.5 mmol) was added with stirring, followed by 10 mL (75 mmol) of 4-methylstyrene. This mixture was then refluxed for 45 h and allowed to cool. Dry, powdered potassium carbonate (1.322 g, 9.6 mmol) was added, and the mixture was stirred for 1 h before being filtered. The filtrate was concentrated in vacuo and purified by chromatography on silica gel in 20% ethyl acetate/hexanes. *p*-Methylphenyldiazene **14b** (1.012 g, 3.78 mmol, 79%) was isolated as a white powder.

The spectral data were:  $^1\text{H}$  NMR (200 MHz,  $\text{CDCl}_3$ ) 7.05 (d, 2H), 6.85 (d, 2H), 2.92 (dd, 1H), 2.30 (s, 3H), 2.02 (dd, 1H), 1.75 (s, 3H), 1.6–1.4 (m, 6H), 1.55 (s, 3H), 1.42 (dd, 1H), 1.3–1.15 (m, 2H);  $^{13}\text{C}$  APT 136.4 (quat), 135.7 (quat), 128.9 (tertiary), 128.8 (tertiary), 90.5 (quat), 89.98 (quat), 67.6 (quat), 47.3 (tertiary), 37.6 (secondary), 28.3 (secondary), 26.8 (secondary), 26.6 (secondary), 26.3 (secondary), 20.97 (primary), 13.5 (primary), 11.4 (primary); MS (CI,  $\text{CH}_4$ ) 269, 267, 240, 225, 151 (base peak), 105; HRMS (CI,  $\text{CH}_4$ ) 269.2007 obsd, 269.2018 calcd for  $\text{C}_{18}\text{H}_{25}\text{N}_2$  ( $\text{M} + \text{H}$ ) $^+$ .

**1,4-Dimethyl-anti-5-(4-bromophenyl)-2,3-diazaspiro[bicyclo[2.2.1]heptane-7,1'-cyclopentan]-2-ene (*p*-Bromophenyldiazene **14e**).** Isopyrazole **13** (0.787 g, 5.24 mmol) was dissolved in 14 mL of  $\text{CHCl}_3$  and purged with nitrogen. Trifluoroacetic acid (0.4 mL, 5.2 mmol) was added with stirring, followed by 10 g (55 mmol) of 4-bromostyrene. The mixture was refluxed under nitrogen for 4 days and then allowed to cool. Powdered dry  $\text{K}_2\text{CO}_3$  (1.046 g, 7.6 mmol) was added and allowed stir for 1.5 h before the mixture was filtered. The filtrate was concentrated in vacuo and chromatographed on silica gel with 20% ethyl acetate/hexanes to yield 0.982 g (2.95 mmol, 59%) of the diazene **14e**.

The spectral data were:  $^1\text{H}$  NMR (200 MHz,  $\text{CDCl}_3$ ) 7.37 (m, 2H), 6.85 (m, 2H), 2.90 (dd, 1H), 2.05 (dd, 1H), 1.75 (s, 3H), 1.6 (m, 2H), 1.52 (s, 3H), 1.5–1.4 (m, 4H), 1.32 (dd, 1H), 1.25–1.18 (m, 2H);  $^{13}\text{C}$  APT 137.9 (quat), 131.1 (tertiary), 130.7 (tertiary), 90.1 (quat), 47.2 (tertiary), 37.6 (secondary), 28.2 (secondary), 26.8 (secondary), 26.6 (secondary), 26.3 (secondary), 13.5 (primary), 11.3 (primary); MS (CI,  $\text{CH}_4$ ) 335, 333, 304, 302, 291, 289, 179, 151 (base peak); HRMS (CI,  $\text{CH}_4$ ) 331.0820 obsd, 331.0810 calcd for  $\text{C}_{17}\text{H}_{20}\text{N}_2\text{Br}$  ( $\text{M} - \text{H}$ ) $^+$ .

**1,4-Dimethyl-anti-5-(4-ethoxycarbonylphenyl)-2,3-diazaspiro[bicyclo[2.2.1]heptane-7,1'-cyclopentan]-2-ene (*p*-Ethoxycarbonylphenyldiazene **14d**).** A round-bottomed flask equipped with a magnetic stirrer was oven-dried and allowed to cool under nitrogen. The flask was charged with 100 mL of dry THF and 1.209 g (3.63 mmol) of *p*-bromophenyl diazene **14e**. The solution was stirred and chilled in a dry ice/acetone bath. To the cold solution was added 8 mL of a 1 M solution of *tert*-butyllithium and the mixture allowed to stir. After 1 h, 7 mL (7.9 g, 73 mmol) of ethyl chloroformate was added in one portion. The solution was then allowed to come to room temperature. TLC on silica gel with 20% (v/v) ethyl acetate/hexanes showed two spots with a positive indication to the  $\text{CuCl}$  diazene stain. The solution was concentrated in vacuo and then quenched with  $\text{K}_2\text{CO}_3$  in ethanol. The products were isolated via chromatography on silica gel in 20% ethyl

acetate/hexanes to yield 0.312 g (0.96 mmol, 26%) of *p*-ethoxycarbonylphenyldiazene **14d**.

The spectral data were:  $^1\text{H}$  NMR (400 MHz,  $\text{CDCl}_3$ )  $\delta$  7.89 (m, 2H), 7.04 (m, 2H), 4.35 (q,  $J = 7.2$ , 2H), 3.00 (dd,  $J = 9.2, 5.4$ , 1H), 2.05 (dd,  $J = 13.6, 9.2$ , 1H), 1.77 (s, 3H), 1.60–1.43 (m, 5H), 1.53 (s, 3H), 1.41 (t,  $J = 7.2$ , 3H), 1.39–1.20 (m, 4H);  $^{13}\text{C}$  NMR (100 MHz,  $\text{CDCl}_3$ ) 166.5, 144.2, 129.2, 129.0, 128.9, 90.5, 90.0, 67.6, 60.8, 47.6, 37.3, 28.2, 26.7, 26.5, 26.2, 14.3, 13.4, 11.3; IR (neat) 2961, 1714, 1275, 1108; MS (CI,  $\text{CH}_4$ ) 327, 298, 283, 151 (base peak), 131; HRMS (CI,  $\text{CH}_4$ ) 327.2068 obsd, 327.2073 calcd for  $\text{C}_{20}\text{H}_{27}\text{N}_2\text{O}_2$  ( $\text{M} + \text{H}$ ) $^+$ .

**1,4-Dimethyl-anti-5-(trimethylsilylmethylene)-2,3-diazaspiro[bicyclo[2.2.1]heptane-7,1'-cyclopentan]-2-ene (Trimethylsilyldiazene **17**).** Isopyrazole **13** (1.405 g, 9.4 mmol) was dissolved in 25 mL of dry, pentene-stabilized chloroform. Allyltrimethylsilane (17 mL, 140.5 mmol) and 0.65 mL (8.43 mmol) of trifluoroacetic acid were added, and the system was nitrogen purged. The mixture was heated to reflux with stirring and allowed to reflux for 2 days before being allowed to cool to room temperature. Powdered dry  $\text{K}_2\text{CO}_3$  (2.44 g, 18 mmol) was added and the mixture allowed to stir for 30 min. The mixture was filtered, solvents were removed under vacuum, and the crude product was chromatographed on silica gel in 4:1 hexanes/ethyl acetate. Trimethylsilyldiazene **17** was isolated (1.684 g, 6.38 mmol, 68%) as a white powder.

The spectral data were:  $^1\text{H}$  NMR (200 MHz) 1.70 (m, 2H), 1.60 (s, 3H), 1.59 (s, 3H), 1.43 (m, 4H), 1.29 (m, 2H), 1.16 (m, 2H), 0.79 (dd, 1H), 0.60 (m, 1H), –0.08 (s, 9H);  $^{13}\text{C}$  APT 91.3 (quat), 89.4 (quat), 66.5 (quat), 38.1 (tertiary), 37.5 (secondary), 28.2 (secondary), 27.1 (secondary), 26.8 (secondary), 26.5 (secondary), 16.5 (secondary), 13.8 (primary), 11.3 (primary), –0.8 (primary); IR (neat ATR) 2952, 2871, 1458, 1381, 1245, 839  $\text{cm}^{-1}$ ; MS (CI,  $\text{CH}_4$ ) 265, 249, 236, 223, 179, 151 (base peak), 73; HRMS (CI,  $\text{CH}_4$ ) 265.2089 obsd, 265.2100 calcd for  $\text{C}_{15}\text{H}_{29}\text{N}_2\text{Si}$  ( $\text{M} + \text{H}$ ) $^+$ .

**1,4-Dimethyl-anti-2-phenylspiro[bicyclo[2.1.0]pentane-5,1'-cyclopentane] (Phenylhousane **10a**).** Diazene **14a** (1.259 g, 4.95 mmol) was weighed into a 250 mL Pyrex round-bottomed flask and dissolved in 50 mL of dry tetrahydrofuran (distilled from Na/benzophenone). The system was degassed by bubbling argon through it for 10 mins. The solution was then irradiated with 365 nm light from a UV hand lamp placed adjacent to the flask, with periodic monitoring by TLC in 4:1 hexanes/ethyl acetate. After 20 h, no more diazene was observed. The solvent was then removed under vacuum, and the crude product was chromatographed on silica gel with cyclohexane. Housane **10a** (1.120 g) was isolated as a clear, viscous liquid (4.95 mmol, >95%).

The spectral data were:  $^1\text{H}$  NMR (400 MHz,  $\text{CDCl}_3$ ) 7.4–7.15 (m, 5H), 2.84 (dd, 1H), 2.09 (dd, 1H), 1.88 (dd, 1H), 1.85–1.65 (m, 6H), 1.45–1.4 (m, 2H), 1.20 (s, 3H), 0.73 (s, 3H); NOE enhancements were observed: irradiated at 2.84 ppm, enhancements at 7.30, 8.3%, 2.08, 2.4%, 1.87, 2.1%, 1.82, 5.9%, 0.73, 0.7%, irradiation at 2.08, afforded enhancements at 2.84, 3.8%, 1.87, 23%, 1.82, 4.9%, 1.2, 0.5%, irradiation at 1.87, afforded enhancements at 7.30, 5.9%, 2.84, 1.7%, 2.08, 21%, 1.2, 2.3%;  $^{13}\text{C}$  APT 145.5 (quat), 128.7 (tertiary), 128.3 (tertiary), 125.98 (tertiary), 42.9 (tertiary), 36.7 (secondary), 29.0 (secondary), 27.1 (secondary), 25.7 (secondary), 24.9 (secondary), 12.9 (primary), 9.2 (primary); MS (EI) 226, 211 (base peak), 169, 115, 91, 41; HRMS (EI) 226.1713 obsd, 226.1722 calcd for  $\text{C}_{17}\text{H}_{22}$   $\text{M}^+$ .

**1,4-Dimethyl-anti-2-(4-methylphenyl)spiro[bicyclo[2.1.0]pentane-5,1'-cyclopentane] (*p*-Methylphenylhousane **10b**).** Diazene **14b** (0.9660 g, 3.60 mmol) was dissolved in 70 mL of dry THF and stirred while being purged with nitrogen. The solution was then irradiated with 365 nm light from a UV handlamp placed against the flask with monitoring by TLC in 4:1 hexanes/ethyl acetate. After 24 h, no more diazene was observed. The solution was concentrated in vacuo and chromatographed on silica 66 gel with cyclohexane as eluent to

yield 0.762 g of 4-methylphenyl housane **10b** (3.175 mmol, 88%) as a clear liquid.

The spectral data were:  $^1\text{H}$  NMR (200 MHz,  $\text{CDCl}_3$ ) 7.25 (m, 4H), 2.92 (t, 1H), 2.45 (s, 3H), 2.19 (dd, 1H), 1.95 (dd, 1H), 1.9–1.7 (m, 6H), 1.6–1.45 (m, 2H), 1.30 (s, 3H), 0.86 (s, 3H);  $^{13}\text{C}$  APT 142.3 (quat), 135.3 (quat), 128.9 (tertiary), 128.4 (tertiary), 42.4 (tertiary), 36.7 (secondary), 28.98 (secondary), 27.1 (secondary), 25.6 (secondary), 24.8 (secondary), 21.2 (primary), 12.9 (primary), 9.1 (primary); MS (EI) 240, 225 (base peak), 197, 183, 105, 91; HRMS (EI) 240.1884 obsd, 240.1878 calcd for  $\text{C}_{18}\text{H}_{24}\text{M}^+$ .

**1,4-Dimethyl-anti-2-(4-methoxyphenyl)spiro[bicyclo[2.1.0]pentane-5,1'-cyclopentane] (p-Methoxyphenyl-housane 10c).** Diazene **14c** (0.575 g, 2.02 mmol) was dissolved in 40 mL of dry THF and stirred while purging with nitrogen. The solution was irradiated with 365 nm light from a UV handlamp placed against the flask with monitoring by TLC in 4:1 hexanes/ethyl acetate. After 25 h, no more diazene was observed. The solution was concentrated in vacuo, and the crude product was chromatographed on silica in 4:1 hexanes/ethyl acetate. Housane **10c** was isolated as a clear, viscous liquid (0.475 g, 1.86 mmol, 92%).

The spectral data were:  $^1\text{H}$  NMR (400 MHz,  $\text{CDCl}_3$ )  $\delta$  7.19 (m, 2H), 6.89 (m, 2H), 3.82 (s, 3H), 2.79 (dd,  $J = 5.0, 4.0$ , 1H), 2.06 (dd,  $J = 11.4, 5.5$ , 1H), 1.86–1.60 (m, 7H), 1.40 (m, 1H), 1.18 (s, 3H), 0.72 (s, 3H);  $^{13}\text{C}$  APT 157.7, 137.4, 129.2, 113.5, 55.22, 41.8, 38.2, 36.7, 33.0, 28.8, 28.9, 26.9, 25.5, 24.5, 12.8, 9.0; MS (EI) 256, 241 (base peak), 213, 199, 121, 91, 41; HRMS (EI) 256.1834 obsd, 256.1827 calcd for  $\text{C}_{18}\text{H}_{24}\text{O}_2\text{M}^+$ .

**1,4-Dimethyl-anti-2-(4-bromophenyl)spiro[bicyclo[2.1.0]pentane-5,1'-cyclopentane] (p-Bromophenylhousane 10e).** Diazene **14e** (0.467 g, 1.40 mmol) was dissolved in 50 mL of dry THF and purged with argon. The solution was then irradiated with 365 nm light from a UV handlamp placed against the flask with periodic monitoring by TLC in 4:1 hexanes/ethyl acetate. After 25 h, no more diazene was detected and the mixture was concentrated in vacuo. The crude product was chromatographed on silica with cyclohexane. The product was then concentrated in vacuo to yield *p*-bromophenylhousane **10e** (0.396 g, 1.30 mmol, 93%).

The spectral data were:  $^1\text{H}$  NMR (500 MHz,  $\text{CDCl}_3$ ) 7.42 (m, 2H), 7.15 (m, 2H), 2.78 (dd, 1H), 2.05 (dd, 1H), 1.8–1.6 (m, 8H), 1.36 (m, 2H), 1.15 (s, 3H), 0.69 (s, 3H);  $^{13}\text{C}$  NMR 144.3, 131.1, 130.1, 127.98, 119.4, 42.2, 38.3, 36.5, 32.7, 28.8, 26.9, 25.4, 24.6, 12.7, 8.95; MS (EI) 306, 304, 291, 289 (base peak), 168, 122, 93; HRMS (EI) 304.0837 obsd, 304.0827 calcd for  $\text{C}_{17}\text{H}_{21}\text{BrM}^+$ .

**1,4-Dimethyl-anti-2-(4-ethoxycarbonylphenyl)spiro[bicyclo[2.1.0]pentane-5,1'-cyclopentane] (p-Ethoxycarbonylphenylhousane 10d).** A round-bottomed flask equipped with a stirbar was charged with 40 mL of distilled THF and 0.284 g (0.87 mmol) of *p*-ethoxycarbonyldiazene **14d**. The solution was degassed by bubbling nitrogen through it for 10 min as it stirred. The flask was then irradiated with nominally 365 nm light from a UV hand lamp placed against the flask for 25 h. The solution was concentrated in vacuo and chromatographed on silica gel in 10% (v/v) ethyl acetate/hexanes to yield 0.098 g (0.33 mmol, 38%) of *p*-ethoxycarbonylphenylhousane **10d**.

The spectral data were:  $^1\text{H}$  NMR (400 MHz,  $\text{CDCl}_3$ )  $\delta$  8.02 (m, 2H), 7.31 (m, 2H), 4.37 (q,  $J = 7.1$ , 2H), 2.89 (dd,  $J = 5.1, 5.1$ , 1H), 2.08 (dd,  $J = 11.5, 5.5$ , 1H), 1.85 (dd,  $J = 11.5, 3.8$ , 1H), 1.82–1.60 (m, 6H), 1.42–1.34 (m, 2H), 1.4 (t,  $J = 7.1, 3\text{H}$ ), 1.19 (s, 3H), 0.70 (s, 3H);  $^{13}\text{C}$  NMR (100 MHz,  $\text{CDCl}_3$ ) 166.7, 150.9, 129.4, 128.3, 126.1, 60.7, 42.8, 38.3, 36.3, 32.7, 28.8, 28.3, 26.9, 25.4, 24.7, 14.4, 12.7, 9.0 IR (neat) 2952, 1718, 1273, 1105; MS (EI) 298, 283, 253, 122, 93 (base peak), 77; HRMS (EI) 298.1936 obsd, 298.1933 calcd for  $\text{C}_{20}\text{H}_{26}\text{O}_2\text{M}^+$ .

**1,4-Dimethyl-anti-2-(trimethylsilylmethylene)spiro[bicyclo[2.1.0]pentane-5,1'-cyclopentane] (Trimethylsilylmethylhousane 11).** Diazene **17** (0.593 g, 2.25 mmol) was dissolved in 50 mL of dry THF in a 125 mL round-

bottomed flask and was stirred while being purged with nitrogen. The solution was irradiated with 365 nm light from a UV hand lamp. After 24 h, no diazene was detected via TLC, and the mixture was concentrated in vacuo. The crude material was chromatographed on silica gel in cyclohexane; the desired fraction was concentrated in vacuo to obtain 0.375 g of trimethylsilylmethyl housane **11** (1.59 mmol, 71%).

The spectral data were:  $^1\text{H}$  NMR (500 MHz,  $\text{CDCl}_3$ ) 1.82 (dd, 1H), 1.63 (m, 1H), 1.69–1.55 (m, 6H), 1.40–1.30 (m, 2H), 1.13 (dd, 1H), 1.01 (s, 3H), 0.94 (s, 3H), 0.80 (dd, 1H), 0.60 (m, 1H), –0.02 (s, 9H);  $^{13}\text{C}$  APT 37.6 (quat), 37.1 (secondary), 33.2 (quat), 33.2 (quat), 31.5 (tertiary), 28.7 (secondary), 26.9 (secondary), 25.5 (secondary), 24.4 (secondary), 21.9 (secondary), 13.6 (primary), 7.8 (primary), –0.8 (primary); MS (EI) 236, 221, 149, 122, 73 (base peak); HRMS (EI) 236.1962 obsd, 236.1960, calcd for  $\text{C}_{15}\text{H}_{28}\text{SiM}^+$ .

**3,7a-Dimethyl-2-phenyl-2,4,5,6,7,7a-hexahydro-1H-indene and 3,7a-Dimethyl-1-phenyl-2,4,5,6,7,7a-hexahydro-1H-indene (Phenylbicyclononene 18 and 19).** Housane **10a** (185 mg, 0.82 mmol) and 1 drop (~8.5 mg, ~0.04 mmol) of 2,6-di-*tert*-butylpyridine were dissolved in 5 mL of dry methylene chloride. This solution was passed through a short column of oven-dried basic alumina into an argon-purged, flame-dried 25 mL flask. The column was then washed with an additional 5 mL of  $\text{CH}_2\text{Cl}_2$ . Tris(4-bromophenyl)aminium hexachloroantimonate (60 mg, 0.07 mmol) was weighed out and dissolved in 5 mL of dry  $\text{CH}_2\text{Cl}_2$ . This solution was then added dropwise, with stirring, via cannula to the housane solution. The mixture was allowed to stir for 5 min before being filtered through a short column of oven-dried basic alumina that was then washed with 5 mL of  $\text{CH}_2\text{Cl}_2$ . Solvents were removed in vacuo, and the crude mixture was chromatographed over silica gel with cyclohexane as eluent. This was followed by removal of the solvent to afford a clear, viscous oil that was pure by HPLC on silica in cyclohexane (HPLC, 7.00 min retention time) in quantitative yield. Subsequent runs were chromatographed in hexanes, and isomers **18** and **19** were separated.

The spectral data for isomer **18** were:  $^1\text{H}$  NMR (500 MHz,  $\text{CDCl}_3$ ) 7.4–7.2 (m, 5H), 3.68 (dd, 1H), 2.42 (m, 1H), 2.20 (dd, 1H), 2.00 (m, 1H), 1.84 (m, 1H), 1.70–1.55 (m, 4H), 1.46 (s, 3H), 1.40–1.25 (m, 1H), 1.25–1.17 (m, 1H), 1.13 (s, 3H); NOE enhancements were observed: irradiated at 7.2 ppm, enhancements at 3.68, 2.5%, 1.46, 0.8%, 1.13, 1%, irradiation at 3.68, afforded enhancements at 7.15, 4.5%, 2.20, 3.6%, 1.46, 1.4%, irradiation at 2.46, afforded enhancements at 2.00, 13%, 1.84, 4.5%, 1.46, 3.5%, irradiation at 2.20, afforded enhancements at 3.68, 3.1%, 1.65, 13%, 1.35, 3.5%;  $^{13}\text{C}$  NMR 147.1, 143.7, 128.9, 128.5, 128.1, 127.96, 125.8, 54.5, 49.5, 47.2, 42.4, 30.3, 28.2, 25.5, 24.0, 23.1, 14.3, 12.6; MS 70 (EI) 226, 211 (base peak), 183, 169, 91; HRMS (EI) 226.1726 obsd, 226.1722 calcd for  $\text{C}_{17}\text{H}_{22}\text{M}^+$ .

The spectral data for isomer **19** were:  $^1\text{H}$  NMR (500 MHz,  $\text{CDCl}_3$ ) 7.35–7.20 (m, 5H), 3.10 (dd, 1H), 2.77 (dd, 1H), 2.42 (m, 1H), 2.30 (dd, 1H), 1.82 (m, 4H), 1.67 (s, 3H), 1.65–1.55 (m, 2H), 1.40 (dd, 1H), 0.58 (s, 3H); NOE enhancements were observed: irradiated at 3.10 ppm, enhancements at 7.3, 4.9%, 2.30, 3.8%, 1.40, 4.0%, irradiation at 2.77, afforded enhancements at 7.3, 9.9%, 2.30, 20.5%, 1.67, 1.7%, 0.58, 1.8%, irradiation at 2.42, afforded enhancements at 1.82, 19.6%, 1.67, 3.6%, irradiated at 2.30, afforded enhancements at 3.10, 4.0%, 2.77, 17.1%, 1.67, 2.4%, irradiation at 0.58, afforded enhancements at 7.3, 6.0%, 2.77, 3.9%, 1.82, 10.6%, 1.40, 7.63%;  $^{13}\text{C}$  APT 141.8 (quat), 139.9 (quat), 128.9 (tertiary), 127.96 (tertiary), 126.2 (quat), 126.1 (tertiary), 57.8 (tertiary), 49.4 (quat), 41.1 (secondary), 39.9 (secondary), 26.9 (secondary), 23.8 (secondary), 22.6 (secondary), 18.5 (primary), 13.8 (primary); IR (neat, ATR) 3026, 2923, 2844, 1601, 1495, 1453, 769, 699  $\text{cm}^{-1}$ ; MS (EI) 226, 211 (base peak), 183, 169, 91; HRMS (EI) 226.1729 obsd, 226.1722 calcd for  $\text{C}_{17}\text{H}_{22}\text{M}^+$ .

**Acid-Catalyzed Test Reaction.** To ensure that the products were not formed via an acid-promoted rearrangement of



the housane, a control experiment was conducted. Phenylhousane **10a** (216 mg, 0.95 mmol) was added to two drops (~58 mg, 0.4 mmol) of 70% aqueous perchloric acid in 11 mL of 10:1 (v/v) CH<sub>3</sub>CN/CH<sub>2</sub>Cl<sub>2</sub> and stirred for 20 h. It is noteworthy that the time required for this reaction was markedly longer than that associated with the electron-transfer processes. The reaction was then quenched with NaHCO<sub>3</sub>, filtered, and concentrated in vacuo. The crude reaction mixture was chromatographed on silica gel with cyclohexane as the eluent. GC/MS analysis indicated the presence of six products, two of which corresponded to **18** and **19**, the products of the electron-transfer induced process. The product ratios, listed in the order in which they eluted, were 55 (adduct **18**): 12:3:2:4:24 (adduct **19**). Neither the number of components, nor the ratio of **18** to **19**, matched the results of the aminium ion promoted process.

**3,7a-Dimethyl-2-(4-methoxyphenyl)-2,4,5,6,7,7a-hexahydro-1H-indene (p-Methoxyphenylbicyclononenes **25** and **26** (X = OMe)).** *p*-Methoxyphenylhousane **10c** (0.393 g, 1.54 mmol) and 1 drop (~8.5 mg, ~0.04 mmol) of 2,6-di-*tert*-butylpyridine were dissolved in 5 mL of dry methylene chloride. This solution was passed through a short column of oven-dried basic alumina into an argon-purged, flame-dried 25 mL flask. An additional 5 mL of CH<sub>2</sub>Cl<sub>2</sub> was then passed through the column into the flask. Tris(4-bromophenyl)aminium hexachloroantimonate (0.129 g, 0.16 mmol) was dissolved in 5 mL of CH<sub>2</sub>Cl<sub>2</sub>, added to the reaction flask dropwise via cannula, and allowed to stir for 1 h. The reaction mixture was then passed through a short column of oven-dried basic alumina and concentrated in vacuo. In 100% petroleum ether, the isomers displayed a nearly identical *R*<sub>f</sub> of 0.2. Nevertheless, they could be separated by painstaking chromatography on a 2 cm diameter column that was loaded with 20 cm of silica gel and eluted with 100% petroleum ether; the products were collected in ~8 mL fractions.

The spectral data for the major product, **25** (X = OMe), were: <sup>1</sup>H NMR (400 MHz, CDCl<sub>3</sub>) δ 7.07 (m, 2H), 6.83 (m, 2H), 3.80 (s, 3H), 3.62 (dd, *J* = 10.3, 4.0, 1H), 2.41 (m, 1H), 2.17 (dd, *J* = 13.4, 10.3, 1H), 2.01 (m, 1H), 1.83 (m, 1H), 1.70–1.56 (m, 3H), 1.44 (s, 3H), 1.32–1.15 (m, 2H), 1.13 (s, 3H); <sup>13</sup>C NMR (100 MHz, CDCl<sub>3</sub>) 157.6, 143.1, 139.0, 128.5, 128.1, 113.3, 55.2, 53.4, 49.3, 46.8, 42.1, 27.9, 25.3, 23.8, 22.8, 12.3.

The spectral data for the minor product, **26** (X = OMe), were: <sup>1</sup>H NMR (400 MHz, CDCl<sub>3</sub>) δ 7.18 (m, 2H), 6.85 (m, 2H), 3.81 (s, 3H), 3.03 (dd, *J* = 11.1, 7.9, 1H), 2.63–2.74 (m, 1H), 2.41–2.44 (m, 1H), 2.30 (dd, *J* = 14.6, 7.5, 1H), 1.77–1.83 (m, 1H), 1.56–1.69 (m, 2H), 1.18–1.48 (m, 3H), 1.44 (s, 3H), 0.55 (s, 3H); <sup>13</sup>C NMR (100 MHz, CDCl<sub>3</sub>) 157.81, 139.7, 133.6, 129.5, 125.9, 113.1, 56.8, 49.0, 40.9, 39.9, 26.6, 23.6, 22.4, 18.3, 13.6; IR (neat) 2926, 2856, 1509, 1244; MS (EI) 256, 241 (base peak), 213, 199, 121; HRMS (EI) 256.1831 obsd, 256.1827 calcd for C<sub>18</sub>H<sub>24</sub>O M<sup>+</sup>.

**3,7a-Dimethyl-2-(4-methylphenyl)-2,4,5,6,7,7a-hexahydro-1H-indene and 3,7a-Dimethyl-1-(4-methylphenyl)-2,4,5,6,7,7a-hexahydro-1H-indene (p-Methylphenylbicyclononenes **25** and **26** (X = Me)).** *p*-Methylphenylhousane **10b** (0.480 g, 1.80 mmol) and 1 drop (~8.5 mg, ~0.04 mmol) of 2,6-di-*tert*-butylpyridine were dissolved in 5 mL of CH<sub>2</sub>Cl<sub>2</sub> and passed through a short oven-dried basic alumina column into an argon-purged, oven-dried 25 mL round-bottomed flask. An additional 5 mL of CH<sub>2</sub>Cl<sub>2</sub> was then passed through the column into the flask. Tris(4-bromophenyl)aminium hexachloroantimonate (161 mg, 0.20 mmol) was dissolved in 5 mL of CH<sub>2</sub>Cl<sub>2</sub>, added to the reaction flask dropwise via cannula, and allowed to stir for 1.5 h. The reaction mixture was then passed through a short column of oven-dried basic alumina and concentrated in vacuo. The crude product was chromatographed in cyclohexane on silica to yield two products in 0.457 g (1.71 mmol) total yield (95% mass balance).

The spectral data for isomer **25** (X = Me) were: <sup>1</sup>H NMR (500 MHz, CDCl<sub>3</sub>) 7.15–7.05 (m, 4H), 3.65 (dd, 1H), 2.43 (dm, 1H), 2.38 (s, 3H), 2.21 (dd, 1H), 2.05 (td, 1H), 1.84 (m, 1H), 1.71–1.59 (m, 4H), 1.46 (s, 3H), 1.39–1.19 (m, 2H), 1.18 (s,

3H); <sup>13</sup>C APT 143.9 (quat), 143.3 (quat), 135.1 (quat), 129.0 (tertiary), 127.1 (tertiary), 53.9 (tertiary), 49.4 (secondary), 46.97 (quat), 42.2 (secondary), 28.0 (secondary), 25.3 (primary), 23.9 (secondary), 22.9 (secondary), 21.1 (primary), 12.5 (primary); MS (EI) 240, 225 (base peak), 183, 105, 91; HRMS (EI) 240.1871 obsd, 240.1878 calcd for C<sub>18</sub>H<sub>24</sub> M<sup>+</sup>.

The spectral data for isomer **26** (X = Me) were: <sup>1</sup>H NMR (500 MHz, CDCl<sub>3</sub>) 7.38 (m, 2H), 6.93 (m, 2H), 3.04 (dd, 1H), 2.75 (dd, 1H), 2.42 (m, 1H), 2.35 (s, 3H), 2.25 (dd, 1H), 1.90–1.79 (m, 3H), 1.66 (s, 3H), 1.65–1.45 (m, 2H), 1.40–1.15 (m, 2H), 0.55 (s, 3H); MS 73 (EI) 240, 225 (base peak), 183, 105, 91; HRMS (EI) 240.1879 obsd, 240.1878 calcd for C<sub>18</sub>H<sub>24</sub> M<sup>+</sup>.

**3,7a-Dimethyl-2-(4-ethoxycarbonylphenyl)-2,4,5,6,7,7a-hexahydro-1H-indene (p-Ethoxycarbonylphenyl bicyclononenes **25** (X = CO<sub>2</sub>Et) and **26** (X = CO<sub>2</sub>Et)).** A two-necked flask equipped with a magnetic stir bar was oven-dried and allowed to cool under nitrogen. The flask was charged via a short column of oven-dried basic alumina with a solution of 0.087 g (0.29 mmol) of *p*-ethoxycarbonylphenylhousane **10d** and 1 drop (~8.5 mg, ~0.04 mmol) of 2,6-di-*tert*-butylpyridine in 5 mL of distilled methylene chloride. The column was then rinsed with 5 mL of distilled methylene chloride into the reaction flask. The reagent tris(*p*-bromophenyl)aminium hexachloroantimonate was weighed (24 mg, 0.029 mmol) and dissolved in 5 mL of CH<sub>2</sub>Cl<sub>2</sub>. The reagent solution was added to the reaction flask and allowed to stir at room temperature for 4 h. The reaction mixture was then filtered through a short column of oven-dried basic alumina and concentrated in vacuo. The crude product was chromatographed on silica in 10% (v/v) ethyl acetate/hexanes to yield 0.075 g (0.25 mmol, 87%) of an inseparable mixture of bicyclononenes **25** (X = CO<sub>2</sub>Et) and **26** (X = CO<sub>2</sub>Et) which were characterized together. Nevertheless, it was easy to differentiate between the isomers because the benzylic proton that is also allylic resonates at lower field.

The spectral data for the major product **25** (X = CO<sub>2</sub>Et) were: <sup>1</sup>H NMR (400 MHz, CDCl<sub>3</sub>) δ 7.95 (m, 2H), 7.20 (m, 2H), 4.37 (q, *J* = 7.1, 2H), 3.70 (dd, *J* = 10.4, 3.7, 1H), 2.41 (m, 1H), 2.21 (dd, *J* = 13.4, 10.4, 1H), 2.02 (m, 1H), 1.85 (m, 1H), 1.70 (m, 1H), 1.62–1.55 (m, 1H), 1.42 (s, 3H), 1.38 (t, *J* = 7.1, 3H), 1.13–1.35 (m, 3H), 1.10 (s, 3H); <sup>13</sup>C NMR (100 MHz, CDCl<sub>3</sub>) 166.8, 152.5, 144.2, 129.7, 127.9, 127.9, 127.2, 60.7, 54.3, 49.1, 47.1, 42.1, 27.9, 25.2, 23.8, 22.8, 14.4, 12.3; IR (neat) 2929, 2857, 1716, 1275; MS (EI) 298, 283 (base peak), 253, 122, 108; HRMS (EI) 298.1927 obsd, 298.1933 calcd for C<sub>20</sub>H<sub>26</sub>O<sub>2</sub> M<sup>+</sup>.

**3,7a-Dimethyl-1-(trimethylsilylmethyl)-2,4,5,6,7,7a-hexahydro-1H-indene (Trimethylsilylmethylbicyclononenes **27** and **28**).** A round-bottomed flask equipped with a magnetic stir bar was oven-dried and allowed to cool under nitrogen. The flask was fitted with a short column of oven-dried basic alumina that was rinsed with 10 mL of dichloromethane into the flask. The flask was then charged via the alumina column with a solution of 2.360 g of trimethylsilylmethyl housane **11** (10 mmol) and 5 drops (~42.5 mg, ~0.02 mmol) of 2,6-di-*tert*-butylpyridine in 10 mL of distilled methylene chloride. The column was then rinsed with 2 × 5 mL of CH<sub>2</sub>Cl<sub>2</sub> followed by 2 × 10 mL of CH<sub>2</sub>Cl<sub>2</sub> into the flask. In an addition funnel, 0.795 g (0.97 mmol) of tris(*p*-bromophenyl)aminium hexachloroantimonate was dissolved in 30 mL of CH<sub>2</sub>Cl<sub>2</sub> and added dropwise. A slight exotherm was observed. The mixture was allowed to react for 90 min before being filtered through oven-dried basic alumina. The reaction mixture was concentrated in vacuo to afford 1.94 g (8.2 mmol; 82%) obtained as an inseparable mixture of the two isomers **27** and **28**, this despite numerous attempts to effect a separation (silica gel, alumina, C18 reversed-phase HPLC). Consequently, the data reported below corresponds to that of the mixture. The presence of diastereotopic protons renders the assignment of proton NMR resonances particularly difficult. Only in cases where our confidence level is high have specific assignments been made. The product distribution was determined by capillary GC, and by GC mass spectral analyses. Of particular

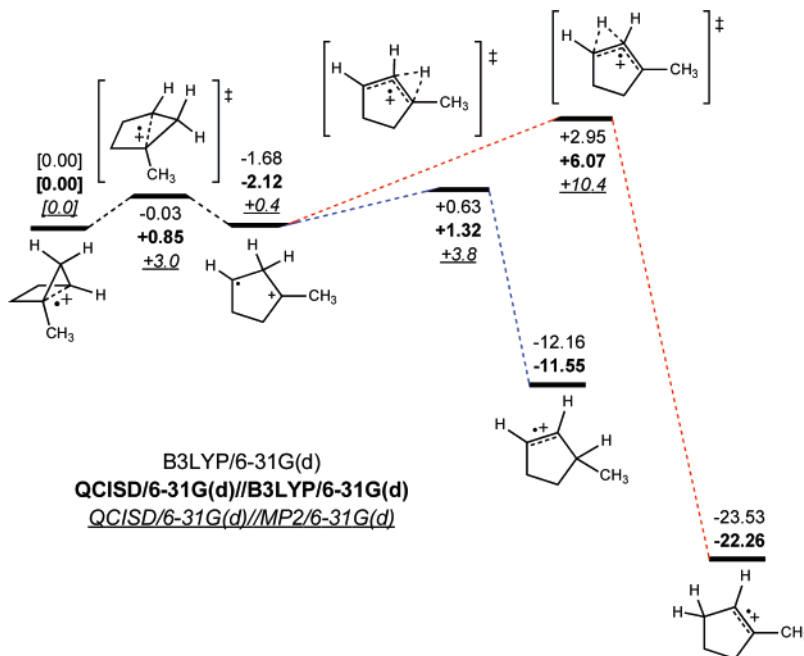


**FIGURE 1.** Rearrangement of methylhousane. Relative energies are in kcal/mol. QCISD/6-31G(d)//MP2/6-31G(d) are from ref 23, while the other values were computed by us.

note is the near identity of the mass spectral fragmentation patterns, thereby confirming the isomeric nature of products. The GCMS data can be found in the Supporting Information.

The spectral data for the mixture of compounds **27** and **28** were:  $^1\text{H}$  NMR (400 MHz,  $\text{CDCl}_3$ )  $\delta$  2.58–2.51 (m, 1H), 2.46–2.28 (m, 2H), 2.05–1.86 (m, 4H), 1.79–1.69 (m, 3H), 1.64 (s, 3H; allylic methyl of one isomer), 1.62 (s, 3H, allylic methyl of the other isomer), 1.60–1.52 (m, 5H), 1.36–1.05 (m, 9H), 1.22 (s, 3H, bridgehead methyl of one isomer), 0.91 (s, 3H, bridgehead methyl of the other isomer), 0.76–0.46 (m, 2H), 0.13 (s, 9H, trimethylsilyl unit of one isomer), 0.12 (s, 9H, trimethylsilyl unit of the other isomer);  $^{13}\text{C}$  NMR (100 MHz,  $\text{CDCl}_3$ )  $\delta$  142.2, 141.3, 139.7, 132.5, 48.6, 48.5, 45.3, 44.4, 44.3, 42.7, 41.0, 34.6, 28.6, 27.6, 26.6, 24.5, 24.3, 23.6, 23.6, 23.2, 17.6, 16.8, 14.1, 12.2, 0.21, 0.32; MS (EI) 236 (molecular ion), 221, 147, 76 73 (base peak); HRMS (EI) 236.1969 obsd, 236.1960 calcd for  $\text{C}_{15}\text{H}_{28}\text{Si}^+$ .

**Computational Methods.** All calculations were performed with GAUSSIAN03.<sup>20</sup> Geometries were optimized using unrestricted B3LYP/6-31G(d).<sup>21</sup> All stationary points were characterized by analysis of their vibrational frequencies. Zero-point energy corrections from these calculations, scaled by

(20) Frisch, M. J.; Trucks, G. W.; Schlegel, H. B.; Scuseria, G. E.; Robb, M. A.; Cheeseman, J. R.; Montgomery, J. A., Jr.; Vreven, T.; Kudin, K. N.; Burant, J. C.; Millam, J. M.; Iyengar, S. S.; Tomasi, J.; Barone, V.; Mennucci, B.; Cossi, M.; Scalmani, G.; Rega, N.; Petersson, G. A.; Nakatsuji, H.; Hada, M.; Ehara, M.; Toyota, K.; Fukuda, R.; Hasegawa, J.; Ishida, M.; Nakajima, T.; Honda, Y.; Kitao, O.; Nakai, H.; Klene, M.; Li, X.; Knox, J. E.; Hratchian, H. P.; Cross, J. B.; Bakken, V.; Adamo, C.; Jaramillo, J.; Gomperts, R.; Stratmann, R. E.; Yazyev, O.; Austin, A. J.; Cammi, R.; Pomelli, C.; Ochterski, J. W.; Ayala, P. Y.; Morokuma, K.; Voth, G. A.; Salvador, P.; Dannenberg, J. J.; Zakrzewski, V. G.; Dapprich, S.; Daniels, A. D.; Strain, M. C.; Farkas, O.; Malick, D. K.; Rabuck, A. D.; Raghavachari, K.; Foresman, J. B.; Ortiz, J. V.; Cui, Q.; Baboul, A. G.; Clifford, S.; Cioslowski, J.; Stefanov, B. B.; Liu, G.; Liashenko, A.; Piskorz, P.; Komaromi, I.; Martin, R. L.; Fox, D. J.; Keith, T.; Al-Laham, M. A.; Peng, C. Y.; Nanayakkara, A.; Challacombe, M.; Gill, P. M. W.; Johnson, B.; Chen, W.; Wong, M. W.; Gonzalez, C.; Pople, J. A. *Gaussian 03*, Revision C.02; Gaussian, Inc: Wallingford, CT, 2004.

(21) (a) Becke, A. D. *J. Chem. Phys.* **1993**, *98*, 5648–5652. (b) Becke, A. D. *J. Chem. Phys.* **1993**, *98*, 1372–1377. (c) Lee, C.; Yang, W.; Parr, R. G. *Phys. Rev. B* **1988**, *37*, 785–789. (d) Stephens, P. J.; Devlin, F. J.; Chabalowski, C. F.; Frisch, M. J. *J. Phys. Chem.* **1994**, *98*, 11623–11627.

0.9806,<sup>22</sup> are included in all reported energies.  $\langle S^2 \rangle$  values for all structures were between 0.75 and 0.78. Despite a bias toward delocalized structures,<sup>1,23,24</sup> the B3LYP method has been used successfully to study the structures and reactions of several different types of cation radicals.<sup>25</sup> In addition, to assess the proficiency of this method for describing rearrangement reactions of housane cation radicals in particular, we examined the rearrangement of the simple methyl-substituted housane shown in Figure 1. Reactions of this species were examined previously using MP2 calculations for geometry optimizations and QCISD single point calculations to assess relative energies of minima and transition state structures.<sup>1,23,26</sup> Figure 1 shows the relative energies of various minima and transition structures involved in the reactions of methyl-substituted housane computed at three different levels of theory. While differing from each other in magnitude, all three methods reproduce the experimentally observed preference for hydrogen migration toward the methyl group.<sup>23,27</sup>

**Acknowledgment.** We are grateful to the National Science Foundation under Grant No. CHE-0200855, for its support of this research. We are also grateful to Professors Barry Carpenter (Cornell) and Jeehiun Lee (Rutgers) for helpful comments. A.B.P. is particularly pleased to acknowledge the ARC Program (Academic Research Consortium), the UC Leads (University of California Leadership Excellence through Advanced

(22) Scott, A. P.; Radom, L. *J. Phys. Chem.* **1996**, *100*, 16502–16513.

(23) Blancfort, L.; Adam, W.; Gonzalez, D.; Olivucci, M.; Vreven, T.; Robb, M. A. *J. Am. Chem. Soc.* **1999**, *121*, 10583–10590.

(24) The Supporting Information for ref 23 points out a specific example of this bias.

(25) (a) Saettel, N.; Oxgaard, J.; Wiest, O. *Eur. J. Org. Chem.* **2001**, 1429–1439. (b) Wiest, O.; Oxgaard, J.; Saettel, N. *J. Adv. Phys. Org. Chem.* **2003**, *38*, 87–110. (c) Fokin, A. A.; Schreiner, P. R. *Chem. Rev.* **2002**, *102*, 1551–1593.

(26) Several recent reviews point to the bias of MP2 calculations towards localized structures as well as its tendency to suffer from spin contamination.<sup>25</sup>

(27) The first B3LYP activation barrier is negative due to the zero point energy corrections; in short, B3LYP predicts that the potential energy surface in the vicinity of the housane cation radical and the 1,3-diyli cation radical is very flat.

Degrees) Program, and the CAMP Program (California Alliance for Minority Participation in Science, Engineering and Mathematics) for supporting his undergraduate research participation in this effort. D.J.T. and S.C.W. are grateful to UC Davis and the National Computational Science Alliance for support.

**Supporting Information Available:**  $^1\text{H}$  and  $^{13}\text{C}$  NMR spectral data, along with coordinates and energies of computed structures. This material is available free of charge via the Internet at <http://pubs.acs.org>.

JO050087C